



Biosorption of Reactive Red 120 Dye from Aqueous Solutions by using Mahagoni (*Swietenia mahagoni*) Wood and Bark Charcoal: Equilibrium, and Kinetic Studies

Tapos Kumar Chakraborty*, Gopal Chandra Ghosh, Mst. Nowshin Akter, Keya Audhikary, Md. Shahnul Islam, Prianka Ghosh, Samina Zaman, Ahsan Habib and A. H. M. Enamul Kabir

Department of Environmental Science and Technology, Jashore University of Science and Technology, P.O. Box 7408, Jashore, Bangladesh.

Received: 05 May 2021, Revised: 15 August 2021, Accepted: 18 September 2021

ABSTRACT

This study analyzed the potential use of Mahagoni wood charcoal (MWC) and Mahagoni bark charcoal (MBC) as biosorbent for reactive red 120 (RR 120) dye removal from aqueous solutions. The effect of different operating parameters such as contact time (1–210 min), pH (3–11), adsorbent dose (1–20 g/L), and initial RR 120 concentration (5–70 mg/L) on adsorption processes was studied under batch adsorption experiments. The maximum removal of RR 120 by MWC (78%) and MBC (88%) was achieved when the optimum conditions were initial RR 120 concentration (5 mg/L), pH (3), adsorbents dose (10 g/L) and equilibrium contact time (150 min). The RR 120 adsorption data of MWC and MBC were better described by the Langmuir and Freundlich isotherm models, respectively. The MWC and MBC showed maximum adsorption capacities of 3.806 and 5.402 mg/g, respectively. Kinetic adsorption data of all adsorbents (MWC and MBC) followed the pseudo-second-order model and this adsorption process was controlled by chemisorption with multi-step diffusion. A lower desorption rate advocated that both strong and weak binding forces could exist between RR 120 molecules and adsorbents. The study results revealed that the utilization of either MWC and or MBC as an adsorbent for treating RR 120 is effective and environmentally friendly.

Keywords: Adsorption efficiency; adsorbent; anionic dye; biomass.

INTRODUCTION

The global trends of industrialization and urbanization have led to releasing numerous toxic chemicals into our environment (Subbaiah & Kim, 2016). Dyes are one of the hazardous toxic chemicals extensively used in different industries including textiles, paint, food, paper, varnishes, ink, plastics, pulp, cosmetics, plastic, and tannery (Subbaiah & Kim, 2016; Abbas et al., 2019). Globally, thousands of commercial dyes are in use and over 7×10^5 tones are manufactured yearly (Munagapati et al., 2017). It is estimated that around 15% of the dyes and pigments are found in effluents, generated from industrial manufacturing and operations steps (Gupta et al., 2012). Discharging of improper/without treatment of colored effluents into water bodies have provoked the altering of aquatic ecosystem stability, because dye obstructs light infiltration through bleaching even at very low concentration, hinders the photosynthetic process, impedes the growth of fauna, generates micro toxin for aquatic organisms, increases chelating of metal ions and chemical oxygen demand (Rápó et al., 2018; Chakraborty et al., 2020). Moreover, dyes itself and their degradation byproduct consider to be toxic, carcinogenic, or even mutagenic, it can also create skin irritation, eye burns, diarrhea to

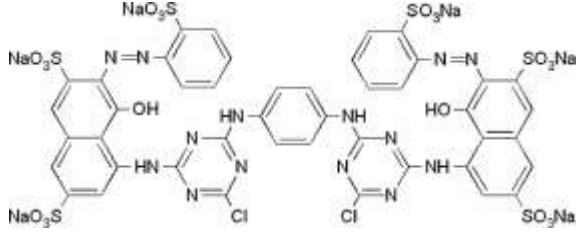
* Corresponding Author: E-mail: taposchakraborty@just.edu.bd

human health (Panda et al., 2009). Based on solubility, dyes are classified into three types: anionic (direct, azo, acid and reactive dyes), cationic (basic dyes) and non-ionic (disperse dyes and vat dyes) (Zheng et al., 2015). Among them, azo dyes are a multipurpose class of organic dyes and incorporating 60–70% of all dyes production (Robinson et al., 2001). Reactive red 120 is an azo dye widely used in various industrial sectors due to its simplicity of application, bright color excellent binding capacity and color swiftness (Eren & Acar, 2006), but its removal is difficult due to distinct properties (e.g. aromatic ring structure, non-biodegradability and highly stable to heat and light) (Subramani & Thinakaran, 2017). Available treatment technologies for dyes removal from wastewater are coagulation and flocculation, membrane separation, ion exchange, reverse osmosis, advanced oxidation processes, oxidation/ozonation, ion exchange, reverse osmosis, photocatalysis, ultrafiltration, electrochemical, adsorption and biosorption (Deng et al., 2011; Yaman & Demirel, 2020). The benefits and drawbacks of each treatment technologies have been broadly reviewed by several authors (Dai et al., 2018; Ghosh et al., 2018; Hasan & Hammood, 2018). Among these technologies, adsorption is the most superior over other technologies in the aspects of cost-effectiveness, low energy input, easy to design and operation, high efficiency, no additional input, the possibility of sorbent regeneration and recovery, and reduction of sludge generation (Dehghani et al., 2017; Anastopoulos et al., 2019). Though commercial adsorbent (e.g. activated carbon as powdered granule) is efficient for dye removal, but it is costly to produce and regenerate. Recently, different types of waste or byproducts of agricultural and forest product are in used as bioadsorbent for removal of dye from wastewater/aqueous solution; such as palm ash (Ahmad et al., 2007), rice husk (Abdelwahab et al., 2005), sugarcane bagasse (Zhang et al., 2013), fly ash (Kumar et al., 2005), almond shell (Duran et al., 2011), jute fiber (Yagub et al., 2014), neem sawdust (Khatti & Singh, 2000), coconut shells (Kadirvelu et al., 2003), etc. bioadsorbent consist of cellulose, proteins and other low molecular weight compounds having different functional groups like carboxyl, hydroxyl, amides, phosphate, which influence the adsorption capacity during adsorption process (Munagapati et al., 2018). Mahagoni is a deciduous tree native to southern Florida, USA and now widely cultivated as a commercial tree in the tropic area. Its leaves, fruits, seeds, bark are used for dye preparation and treatment of many diseases (Ghosh et al., 2020). In this study, MWC and MBC were chosen as adsorbent due to its availability, cost-effectiveness, and eco-friendly criteria. As the best of our knowledge, there is no study on the removal of RR 120 by MWC and MBC. Therefore, the objectives of this study are to investigate the applicability of MWC and MBC for removing RR 120 from aqueous solutions by influencing different experimental parameters; contact time, pH, adsorbent dose, and initial RR 120 concentration. Finally, the adsorption behaviors of MWC and MBC for RR 120 were studied by different kinetics and isotherms model.

MATERIALS AND METHODS

Analytical grade reactive dye (RR 120) was purchased from Sigma-Aldrich, USA. The chemical structure and properties of RR 120 are presented in Table 1. The stock solution of RR 120 (200 mg/L) was prepared by dissolving the required amount of dye powder in double distilled water, and the desired working solution was prepared from the stock solution by successive dilution with double distilled water.

Table 1. Physico-chemical properties of RR 120.

Properties	Reactive Red 120 (RR 120)
Chemical structure	
Molecular formula	C ₄₄ H ₂₄ C ₁₂ N ₁₄ O ₂₀ S ₆ Na
Molecular weight	1469.98 g/mol
CAS Number	61951-82-4
Water solubility	70 g/L
λ_{\max}	535 nm
Class	Diazo (-N=N-board)
Color	Red blue light

MWC was collected from the local area, Jashore, Bangladesh. After collection washed with water to remove the ash and dirty then dried in an oven (Labtech LDO-150F, Korea) at 80°C for 24 h, cooled at room temperature. The dried coal was crushing by a mortar and pestle, and 0.5 to 1.0 mm size particles were collected through the sieve. After that collected particles were kept into the double-distilled water at 20 h, for soaking, again dried in an oven at 80°C for 24 h.

Mahagoni bark was collected from a local sawmill, located in Jashore, Bangladesh. After collection, it cut into small pieces (5 inches long) and washed with water to remove dirt and color. Then further washed with double distilled water and dried in an oven (Labtech LDO-150F, Korea) at 80°C for 24 h, cooled at room temperature. The bark was soaked in 0.1N NaOH solution for 24h to remove excess color, after that dried again in an oven at 80°C for 24 h, carbonized into a muffle furnace (SXT-10, Shanghai Shuli Instrument and Meters Co., Ltd.) at 200°C for 15 min. The carbonized charcoal was washed with double distilled water and further dried in an oven at 80°C for 24 h, crushed by a mortar and pestle, and 0.5 to 1.0 mm size particles were collected through the sieve. Finally, MWC and MBC were stored in airtight borosilicate glass bottles and, used for experiments as needed. FTIR (Fourier Transform Infrared Spectroscopy) spectra of MBC and MWC were recorded before and after adsorption of RR 120 in a spectrometer (FTIR-4600, JASCO Corporation Ltd., Japan). The surface morphology of MWC and MBC was observed before and after adsorption of RR 120 by using a field emission scanning electron microscope (FE-SEM, Zeiss Sigma, Carl Zeiss, Germany).

Adsorption of RR 120 onto MWC and MBC were conducted as functions of contact time (1–210 min), pH value (pH 3–11), adsorbent dose (1–30 g/L), and initial dye concentration (5–70 mg/L) under the batch experiments. The pH of the experiment solution was adjusted by adding 0.1 N HCl / 0.1 N NaOH solutions. Experiments were accomplished with 250 mL of working solution (with appropriate dye concentration and pH) and appropriate adsorbent in 500 mL beaker. These beakers were stirred in the Jar-test instrument (JLT4, VELS Scientifics, Italy). After completion of each experiment, a sufficient amount of suspension was taken from the beaker and filter by a glass microfiber filter paper (GF/B, Whatman, USA) to removing adsorbent particles. The concentration of RR 120 in solution was measured by a

UV-visible spectrophotometer (HACH DR 3900, USA) at 535 nm wavelength. Duplicate experiments were conducted and mean values were applied. The amount of RR 120 adsorption at equilibrium and the percentage of removal were calculated by using Equation 1 and Equation 2, respectively.

$$q_e = \frac{(C_0 - C_e)V}{m_s} \quad (1)$$

$$R (\%) = \frac{(C_0 - C_e)}{C_0} \times 100 \quad (2)$$

Where, C_0 and C_e are the initial and at equilibrium RR 120 concentrations in mg/L, respectively. q_e is the equilibrium RR 120 adsorbed in mg/g. V is the volume of solution (L) and m_s is the mass of adsorbent (g).

The adsorption isotherm experiments were carried out by taking 250 mL of RR 120 solutions with varying initial concentrations (5–70 mg/L) in different 500 mL beaker. The fixed amount of adsorbent (10 g/L g) was added to each beaker and kept the agitation speed at 200 rpm with the optimum pH (3) at room temperature ($25 \pm 2^\circ\text{C}$) and equilibrated contact time for 150 min. In this study, two equilibrium adsorption isotherm models, Langmuir and Freundlich, were used. The Langmuir isotherm is used to predict the maximum monolayer sorption capacity on the external surface of the adsorbent with a fixed number of adsorption sites (Langmuir, 1917). This isotherm model may be represented as in Equation (3).

$$q_e = \frac{q_{max} b C_e}{1 + bC_e} \quad (3)$$

Where C_e is the equilibrium concentration of remaining RR 120 in the solution (mg/L), q_e is the amount of RR 120 adsorbed at equilibrium (mg/g), q_{max} is the amount of RR 120 at complete monolayer coverage (mg/g), and b (L/mg) is Langmuir constant related to adsorption capacity and rater of adsorption. The essential feature of the Langmuir isotherm can be expressed in terms of dimensionless constant separation factor (R_L) that is used to predict whether an adsorption system is “favorable” or “unfavorable” (Nghah and Musa, 1998). The separation factor is presented in Equation (4).

$$R_L = \frac{1}{1 + bC_0} \quad (4)$$

The adsorption process as a function of R_L may be described as $R_L > 1$; unfavorable, $R_L = 1$; Linear, $0 < R_L < 1$; favorable and $R_L = 0$; irreversible.

The Freundlich isotherm describes the heterogeneous adsorption surfaces corresponding with the adsorption intensity of adsorbent (Freundlich, 1906). This isotherm may be represented as in Equation (5).

$$q_e = K_F C_e^{1/n} \quad (5)$$

Where, K_F and n are Freundlich constant and adsorption intensity, respectively. Values of n , represent the adsorption process is to be either poor ($n < 1$), moderately difficult ($1 < n < 2$), or good in ranging from 2 to 10 (Chen et al., 2011), while higher K_F values indicate an easy uptake of dye from the solution.

The adsorption kinetic experiments were conducted by adding 10 g/L adsorbent into 350 mL RR 120 solution (containing 20 mg/L of RR 120 dye concentration) at optimum pH (3) and stirring speed of 200 rpm at room temperature ($25\pm 20^\circ\text{C}$). The samples were collected from the solution after selected time intervals (1, 5, 7, 10, 15, 30, 60, 90, 120, 150, 180, and 210 min), filtered, and analyzed. Adsorption kinetic delivers information on adsorption rate of RR 120 by the adsorbents, retention time required for the adsorption process, and mechanism of reactions. Lagergren pseudo-first-order model (Lagergren, 1898) and Ho's pseudo-second-order model (Ho & McKay, 2000) were used to identify the kinetics behavior, whereas inter-particle diffusion model was used to investigate the diffusion mechanism and potential rate-controlling step in the adsorption process. Lagergren pseudo-first-order model is expressed in Equation (6) and Ho's pseudo-second-order model expressed in Equation (7).

$$q_t = q_e (1 - e^{-k_1 t}) \quad (6)$$

Where, K_1 is the pseudo-first-order rate constant (min^{-1}), q_e , and q_t are the amount of RR 120 adsorbed (mg/g) at equilibrium and time, t .

$$q_t = \frac{K_2 q_e^2 t}{1 + K_2 q_e t} \quad (7)$$

Where, K_2 is the pseudo-second-order rate constant (g/mg/min),

The intraparticle diffusion model was explored by Weber and Morris equation. This model indicates the presence of the intraparticle diffusion of adsorbate in the adsorbent surfaces during the adsorption process (Weber & Morris, 1963). The intraparticle diffusion model is expressed in Equation (8).

$$q_t = K_{diff} \cdot t^{0.5} + C \quad (8)$$

Where K_{diff} is the intraparticle diffusion rate constant ($\text{mg/g min}^{0.5}$), which can be calculated from the slope of a linear plot q_t versus $t^{0.5}$ and C is intercept, which represents the thickness of the boundary layer. If the linear plot passes through the origin, with no intercept then intraparticle diffusion only the rate-limiting step; otherwise not only intraparticle diffusion but also other diffusion mechanisms also involved during adsorption process.

The residual sum square (RSS) and chi-square (χ^2) test were calculated to find the best fit among the used adsorption isotherm and kinetic models (Chahm et al., 2018). Lower error and chi-square value indicate the best fitting of the models. The equation for evaluating the best fit model expressed in Equation (9) and (10).

$$RSS = \sum (q_{exp} - q_{cal})^2 \quad (9)$$

$$\chi^2 = \sum \frac{(q_{exp} - q_{cal})^2}{q_{cal}} \quad (10)$$

Where q_{cal} is the calculated adsorption data (mg/g) from models, q_{exp} is the observed experimental adsorption data (mg/g) from both isotherm and kinetic models.

Additionally, a normalized standard deviation test was used to get the fitting result of kinetic models, which is presented in Equation (11).

$$\Delta q (\%) = 100 \times \frac{\sum [(q_{exp} - q_{cal})/q_{exp}]^2}{n - 1} \quad (11)$$

Where q_{cal} is the calculated adsorption data (mg/g) from models, q_{exp} is the observed experimental adsorption data (mg/g) from the kinetic models and n is the numbers of data points.

For desorption study, RR 120 loaded MWC and MBC were collected from isotherm experiments. The adsorbents were then filtered and dried in the oven at 80°C for 24 h. RR 120 loaded adsorbent was transferred into pH-controlled distilled water (pH 5, 7, 9, and 11) for 150 min at a constant stirring speed of 200 rpm. The amount of dye desorbed was measured percentage of desorption was calculated by Equation (12).

$$Desorption (\%) = \frac{Mass\ of\ dye\ desorbed\ (mg/L)}{Mass\ of\ dye\ adsorbed\ (mg/L)} \times 100 \quad (12)$$

RESULTS AND DISCUSSION

FTIR spectra of MBCs, before and after adsorption of RR120, were shown in Fig. 1(a). The major adsorption region around 3524 cm^{-1} was contributed to O–H stretching vibrations of hydroxyl or carboxyl groups and –NH groups (Mubarak et al., 2017). The adsorption peak at 2987 cm^{-1} could be attributed to the –CH₂ stretching vibrations (Qian et al., 2018). The C=O stretches of the carboxyl group were located at 1745 cm^{-1} peak. The peak around 1629 cm^{-1} was assigned to C=C stretching from the aromatic rings of lignin (Zhu et al., 2015). The band at 1573 cm^{-1} was assigned to –CN stretching vibrations (Çelekli et al., 2012). The adsorption around 1381 cm^{-1} and 1416 cm^{-1} assigned that the asymmetrically and symmetrically stretching vibrations of –CH₃ in the amide group (Rusmin et al., 2015). The adsorption peak at 695–875 cm^{-1} was controlled by aromatic C–H bending vibrations.

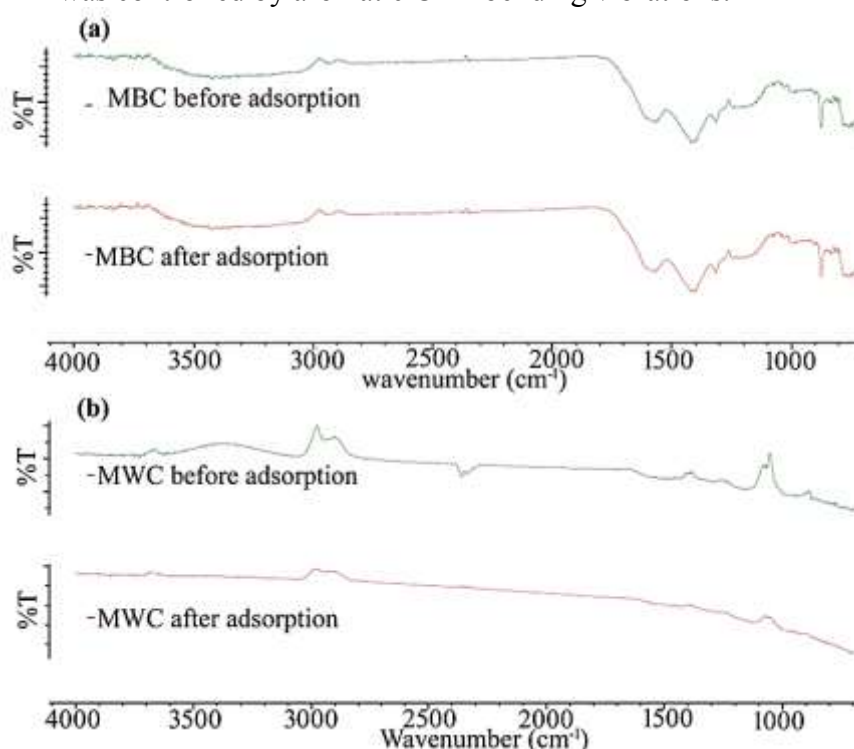


Fig. 1. FTIR spectra of (a) MBC and (b) MWC for the adsorption of RR 120.

Similarly, the before and after adsorption FTIR spectra of MWC could be attributed as follows (Fig. 1(b)): 3750 cm^{-1} (strong band vibration of $-\text{OH}$ and $-\text{NH}$ groups), $3082\text{--}2946\text{ cm}^{-1}$ ($-\text{CH}$ stretching vibrations), 1732 cm^{-1} ($\text{C}=\text{O}$ stretching), 1639 cm^{-1} (amide, NH_2 bending), 1575 cm^{-1} ($-\text{CN}$ stretching), 1220 cm^{-1} ($-\text{C}-\text{N}$ stretching vibrations), $1152\text{--}1071\text{ cm}^{-1}$ ($\text{C}-\text{O}$ vibrations from cellulose and hemicelluloses) and 940 and 873 cm^{-1} ($\text{C}=\text{O}$ and $\text{C}-\text{C}$ stretching vibrations). Finally, the FTIR results showed that hydroxyl, carboxyl, and amine groups were presented on the MBC and MWC surface, and previous studies for adsorption of RR 120 onto *Lentinussajor-caju* (Arica & Bayramoğlu, 2007), *Chara contraria* (Çelekli et al., 2012), chitosan beads (Mubarak et al., 2017) and *Hydrilla verticillate* (Naveen et al., 2011) indicates that these functional groups (hydroxyl, amine, and carboxyl) significantly provoke the adsorption of RR 120.

The surface morphology of MWC and MBC, before and after adsorption of RR 120, were observed by FE-SEM and given in Fig. 2. Before the adsorption of RR 120, the surface of MWC and MBC were irregular and contain larger numbers of different sizes pore, which facilitates large surface area for interaction between RR 120 molecules and adsorbent (Fig. 2(a), 2(c)). However, the surfaces of the adsorbents were saturated by RR 120 molecules after RR 120 adsorption (Fig. 2(b), 2(d)).

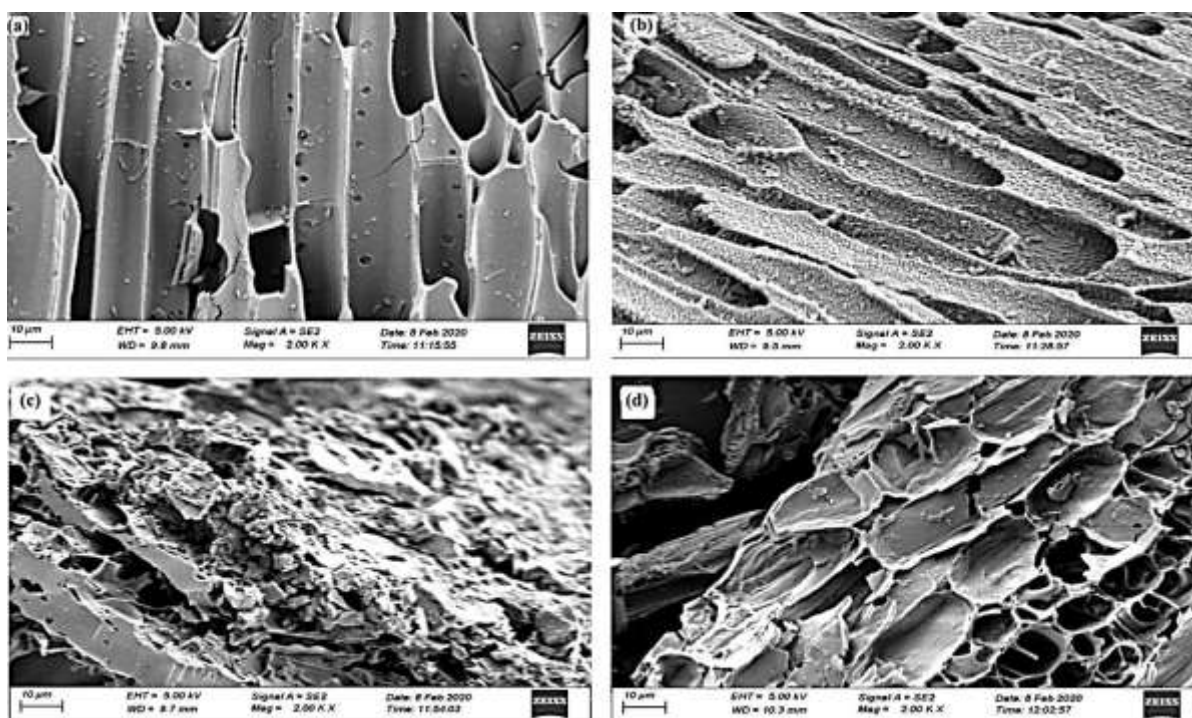


Fig. 2. FE-SEM photographs of MWC (a. before adsorption; b. after adsorption) and MBC (c. before adsorption; d. after adsorption) at 2000 magnifications.

For evaluating the effects of contact time and initial dye concentration on RR 120 adsorption by MWC and MBC, experiments were conducted with different contact times (1–210 min) and initial dye concentrations (5, 20 and 50 mg/L) at $25\pm 2^\circ\text{C}$ temperature under the optimum operating conditions (10 g/L adsorbent dose; pH 3), and 200 rpm stirring speed. As shown in Fig. 3, the adsorption process was controlled by three steps: (1) rapid adsorption found at beginning (0–1 min) due to higher concentration gradient of RR 120 and a large number of available active sites on the adsorbent surface, (2) the adsorption rate became slow (1–150 min) because decreasing of available active sites on the adsorbent surface with time

progress, and (3) the adsorption rate relatively very slow (150–210 min) may be due to the remaining active sites are difficult to be occupied for the repulsive forces between the RR 120 molecules on the adsorbent surface in bulk solution (Shirmardi, 2012).

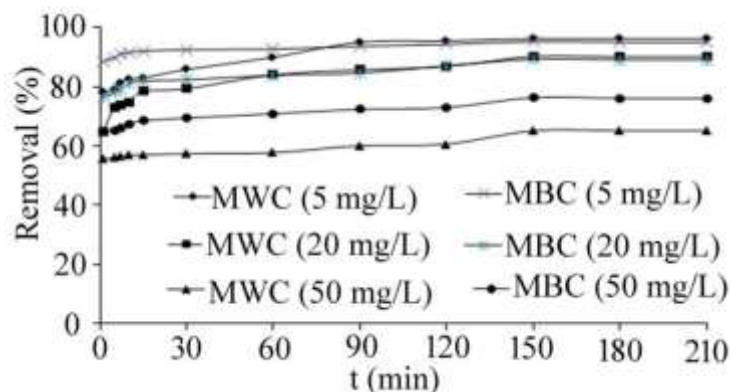


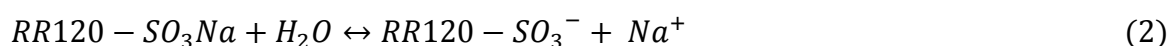
Fig. 3. Effect of contact time and initial RR 120 dye concentration on removal of RR 120 dye by MWC and MBC.

The adsorption equilibrium was reached at 150 min; therefore 150 min was selected for further studies. However, the removal rate of RR 120 decrease with increase initial RR 120 concentration, for example, at each equilibrium time, RR 120 removal percentage by MWC and MBC decreased from 78% to 65% and 88% to 76%, respectively, with an increase initial RR 120 concentration from 5 to 50 mg/L (Fig. 3), because at the constant dose the adsorbent external surface is saturated as well as dye molecules block the pores of the adsorbent. So the removal efficiency significantly depends on the initial RR 120 concentration and contact time.

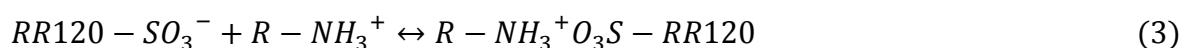
pH plays a significant role in adsorption study, which influence the nature of adsorbate ionization in solution, dissociation of functional groups on the binding sites of adsorbent as well as changing of adsorbent surface charge (Ai et al., 2011). Adsorption behavior of RR 120 onto MWC and MBC at various pH values (ranging from 3 to 11) plotted in Fig. 4(a), indicating that RR 120 adsorption onto MWC and MBC closely depends on solution pH. The removal efficiency of RR 120 decrease (MWC=90–24%, MBC=90–3%) with increasing pH (pH 3–11), and maximum removal was found at pH 3 (90%) for both adsorbents. The reasons are at low pH the concentrations of H^+ are increased in solutions, which may lead to the protonation of the NH_2 functional group present onto the surface of the adsorbent (Arami et al., 2008).



In aqueous solution, the sulfonate group of RR 120 is dissociated and converted to anionic dye ions



So, strong electrostatic attraction between anionic RR 120 molecules and positively charged adsorbent surface leading to the maximum removal



Similar explanation was proposed by (Mubarak et al., 2017) for the removal of RR 120

using chitosan beads. Conversely, the removal efficiency decreased at higher pH due to the increase of competition for adsorption sites between excess OH^- ions and anionic RR120 molecules.

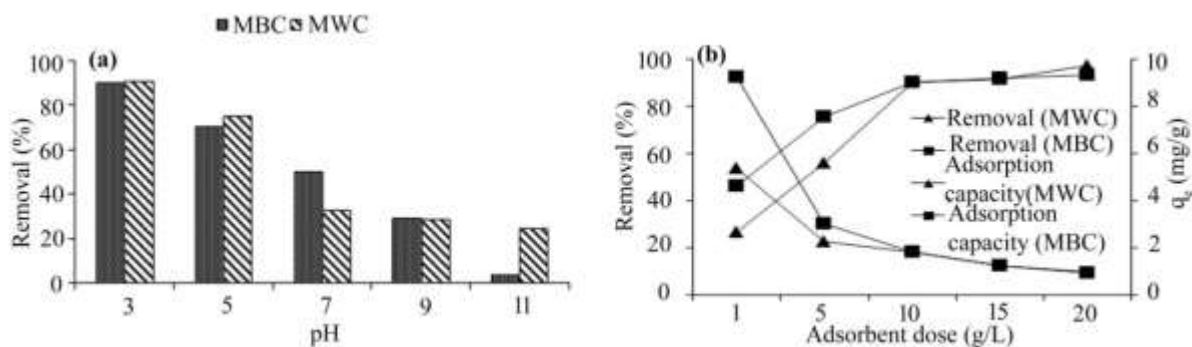


Fig. 4. Effect of (a) pH and (b) adsorbent dose on removal of RR 120 by MBC and MWC.

The adsorbent dose is considered a vital technical parameter, which largely influenced the removal of contaminants from wastewater because it measures the adsorbate adsorption capacity (Deng et al., 2011). The adsorption experiments were conducted with the variation of adsorbent doses (1, 5, 10, 15 and 20 g/L) under the following fixed experimental condition: RR 120 concentration of 20 mg/L, pH 3, temperature $25 \pm 2^\circ\text{C}$, contact time 150 min and stirring speed of 200 rpm. Effect of adsorbent dose on the adsorption process presented in Fig. 4(b), illustrating that RR 120 removal efficiency increased from 26% to 97% and 46% to 93% with increasing MWC and MBC doses (1–20 g/L), respectively. This is due to the higher adsorbent dose creates larger surface areas and more interchangeable sites on the adsorbent surface, achieving higher adsorption efficiency (Jain et al., 2010). However, increased adsorbents dose (1–20 g/L) showed a lower adsorption rate (5.36 to 0.97 mg/g and 9.25 to 0.93 mg/g for MWC and MBC, respectively), this could be the competition or overlapping (e.g. aggregation) of RR 120 molecules onto the adsorption sites (Bansal et al., 2009). Ghosh et al., (2020) found similar trend for removing of anionic dye from aqueous solution by biosorbent.

The equilibrium experimental data of RR 120 adsorption onto MWC and MBC were analyzed by Langmuir and Freundlich isotherms, which are commonly applied in the solid/liquid system presented in Fig. 5(a), 5(b), respectively.

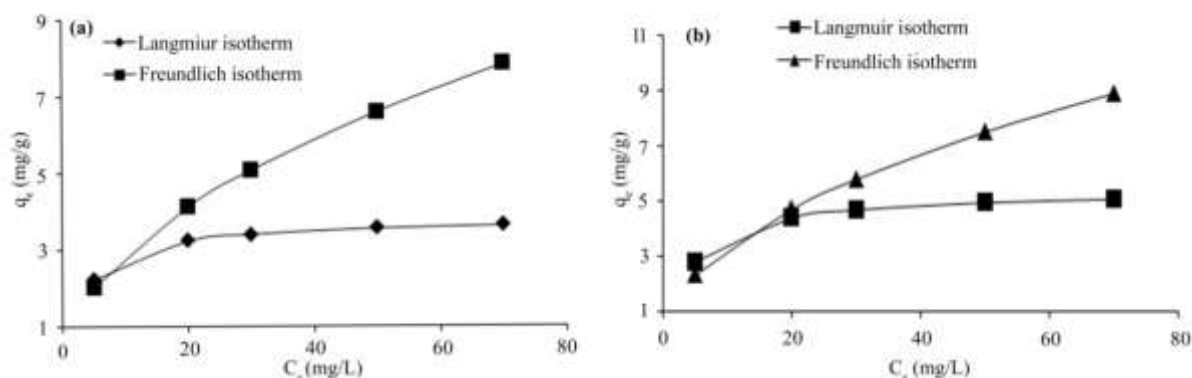


Fig. 5. (a) Langmuir isotherm and (b) Freundlich isotherm models for the adsorption of RR 120 by MWC and MBC.

The best fitted result of isotherms depends on correlation coefficients (R^2), Chi-square (χ^2) and residual sum square (RSS) value, presented in Table 2.

Table 2. Isotherm parameters for adsorption of RR 120 onto MWC and MBC

Isotherm models	Parameters	MWC	MBC
Langmuir	q_{max} (mg/g)	3.806	5.402
	b (L/mg)	0.285	0.215
	R_L	0.411-0.047	0.462-0.062
	R^2	0.991	0.946
	RSS	6.795	18.940
	χ^2	2.508	4.899
Freundlich	K_F (mg/g) (L/mg) ^{1/n}	0.897	1.020
	n	2.329	1.959
	R^2	0.898	0.978
	RSS	13.551	9.124
	χ^2	3.665	3.221

The results showed that higher correlation coefficient value ($R^2=0.991$), lower error (RSS=6.795), and chi-square value ($\chi^2=2.508$) of Langmuir isotherm for adsorption of RR 120 onto MWC was fitted better than Freundlich isotherm ($R^2=0.898$, RSS=13.551 and $\chi^2=3.665$) (Table 2). This indicates that RR 120 molecules create monolayer coverage with homogenous distribution onto MWC. Therefore, Freundlich ($R^2=0.978$, RSS=9.124, and $\chi^2=3.221$) was the best-fit isotherm for the adsorption of RR 120 onto MBC than Langmuir isotherm ($R^2=0.946$, RSS=18.940, and $\chi^2=4.899$) (Table 2), which exhibited that the surface of MBC was not uniform, had nearly heterogeneous sites for RR 120 adsorption. The monolayer maximum adsorption capacity of RR 120 onto MWC and MBC, calculated from the Langmuir isotherm was 3.806 and 5.402 mg/g, respectively (Table 2). However, the adsorption capacities for the MWC and MBC shows potential for the removal of RR 120 from aqueous solutions, with the decreasing order of MBC > MWC. The R_L values of MWC and MBC were calculated from Langmuir isotherm lies within 0 and 1, indicating that RR 120 adsorption onto MWC and MBC was suitable under the conditions studied. On the other hand, the value of adsorption intensity (n) for MWC and MBC obtained from Freundlich isotherm was higher than 1, indicating that the adsorption process was favorable of both MWC and MBC as an adsorbent for RR 120 adsorption from aqueous solutions (Table 2).

In this study, three kinetic models (Lagergren pseudo-first-order, Ho's pseudo-second-order, and intraparticle diffusion) were applied to determine the adsorption behavior of RR 120 onto MWC and MBC, presented in Fig. 6, and the model's parameters values are in Table 3. The higher R^2 and lower values of RSS, Δq (%) and chi-square (χ^2) were calculated from the pseudo-second-order kinetic model for each initial RR 120 concentration than the pseudo-first-order kinetic model, and the calculated ($q_{e,cal}$) values from the pseudo-second-order kinetic model also corresponding with the experimental ($q_{e,exp}$) values for both adsorbents (MWC and MBC) (Table 3), confirming that the adsorption process follows the pseudo-second-order kinetic model. So, the whole adsorption processes seem to be controlled by chemisorption i. e. the electrostatic interactions between the surface of the positively charged adsorbent and negatively charged RR 120 molecules. For both adsorbents, the pseudo-second-order rate constant (K^2) decreased with increasing RR 120 concentration under similar experimental conditions (Table

2), which confirms that lower mass transfer happens at a high dye concentration gradient due to the higher competition for the adsorption sites (Chen et al., 2011).

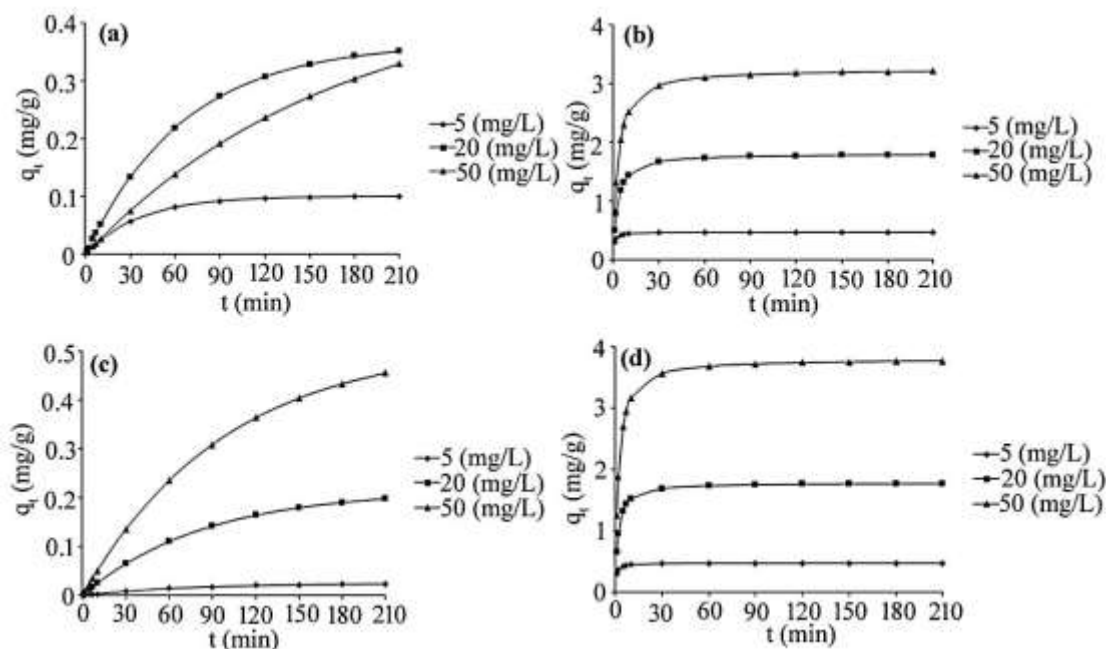


Fig. 6. Kinetic models for the adsorption of RR 120 by MWC (a. Pseudo-first order; b. pseudo-second order kinetic model) and MBC (c. Pseudo-first order; d. pseudo-second order kinetic model).

This could be assigned that diffusion increased on a solid surface than the boundary layer (Deng, 2011). According to the results of Table 2, the adsorption rate of MBC was higher than MWC at every initial RR 120 concentration due to the proper utilization of adsorbent adsorption capacities by the larger driving force at higher concentration gradient. The experimental data were further analyzed by intraparticle diffusion in order to investigate the diffusion mechanisms. The intraparticle diffusion plot did not pass through the origin (Fig. 7(a)) and intercept values (c) were increased with an increase of initial RR 120 concentration (Table 3), indicating that the rate-limiting step of RR 120 adsorption onto MWC and MBC were external diffusion (i.e. agglomerate of RR 120 molecules on the adsorbent surface) than internal diffusion (i. e. transport of RR 120 molecules inside the adsorbent particle), that may occur simultaneously.

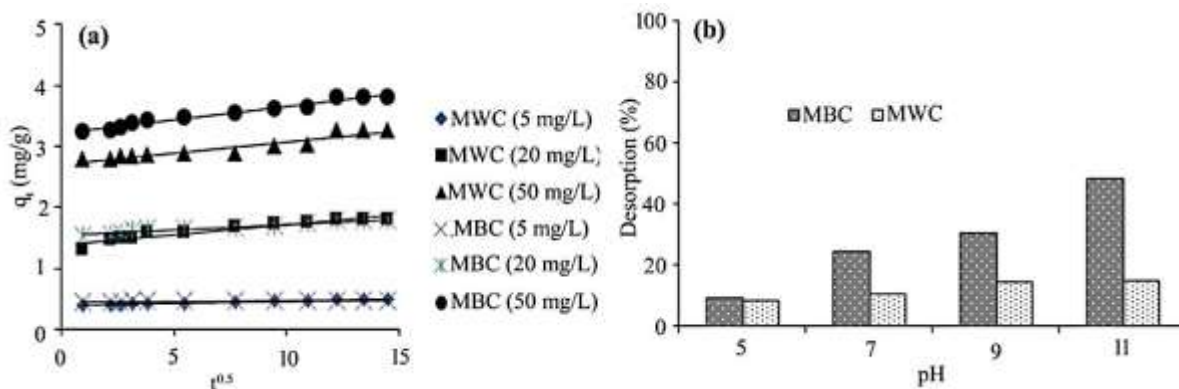


Fig. 7. (a) Intra-particle diffusion plot and (b) desorption of RR 120 by MWC and MBC.

Adsorption capacities of different adsorbents for removal of anionic reactive dyes reported in the literature, given in Table 4. Comparative results indicate that the adsorption capacity of MBC and MWC are moderate and suitable alternative adsorbent for the removal of anionic reactive dyes than other adsorbents from aqueous solutions due to low cost, easily available, environmentally friendly and does not generate secondary pollution.

Table 3. Kinetic parameters for RR 120 adsorption onto MWC and MBC.

Models	Parameters	MWC (initial RR 120 concentration in mg/L)			MBC (initial RR 120 concentration in mg/L)		
		5	20	50	5	20	50
Pseudo-first order	$q_{e,exp}$ (mg/g)	0.480	1.803	3.254	0.475	1.784	3.813
	$q_{e,cal}$ (mg/g)	0.100	0.366	0.461	0.024	0.216	0.518
	K_1 (min ⁻¹)	0.027	0.015	0.006	0.014	0.011	0.010
	R^2	0.963	0.940	0.948	0.913	0.911	0.955
	RSS	1.76	27.22	96.50	2.44	29.94	132.25
	χ^2	124.56	917.05	5828.33	1265.25	2126.99	4309.52
	Δq (%)	95.5	98.1	104.3	106.4	103.2	103.0
Pseudo-second order	$q_{e,cal}$ (mg/g)	0.485	1.814	3.259	0.475	1.787	3.814
	K_2 (g/mg min)	1.001	0.211	0.104	3.412	0.322	0.127
	H (mg/g min)	0.235	0.697	1.110	0.772	1.030	1.854
	R^2	0.999	0.999	0.998	0.999	0.999	0.999
	RSS	0.08	1.93	7.14	0.03	1.25	6.57
	χ^2	0.46	3.07	6.80	0.09	1.63	4.45
	Δq (%)	31.6	14.7	18.7	6.4	13.0	14.35
Intraparticle diffusion	K_{diff} (mg/gmin ^{0.5})	0.007	0.032	0.037	0.002	0.018	0.043
	C (mg/g)	0.386	1.380	2.700	0.447	1.536	3.207
	R^2	0.950	0.916	0.904	0.908	0.951	0.972

Reversibility or desorption process regulated by the strong binding bond (ionic or covalent bonding) or weak binding forces (Van der Waals' forces or a dipole-dipole interaction) between the adsorbent surface and adsorbate molecules (Ip et al., 2009). In this study, the desorption abilities of MBC and MWC were studied at different pH values (pH 5, 7, 9, and 11). Figure 7(b) indicates the desorption percentage of MBC (9–48%) and MWC (8–15%) was low, but between them, the desorption rate of MBC was comparatively high (Fig. 7(b)) because the weak binding forces (Van der Waals attraction and π - π interactions) were dominated between the RR 120 molecules and MBC surface due to increase pH values, as well as more adsorption of RR 120 onto the MBC surface act as a driving force of this desorption. Inversely, MWC showed lower (8–15%) desorption the probable cause was a strong binding bond between RR 120 molecules and MWC surface instead of increasing pH values (Fig. 7(b)). Similar observation also found by other studies (Çelekli et al., 2011; Mahmoodi et al., 2011; Çelekli et al., 2012). This study suggested that both the strong and the weak binding forces could exist between the adsorbents (MBC and MWC) and RR 120 molecules.

Table 4. Comparison of anionic reactive dye adsorption capacity by MWC and MBC with other adsorbents.

Adsorbents	Types of reactive dyes	Maximum adsorption (mg/g)	pH	Contact time (min)	Adsorbent dose (g/L)	Initial dye concentration range (mg/L)	References
Chitosan beads	Reactive red 120	129.9	4.0	180	3.0	30–400	(Mubarak et al., 2017)
Characontraria	Reactive red 120	112.83	1.0	180	1.0	25–200	(Çelekli et al., 2012)
Mahagoni bark coal	Reactive red 120	5.40	3.0	150	10.0	5–70	This study
Alumina/multi-walled carbon nanotubes	Reactive red 198	4.53	3.0	150	0.40	10–200	(Malakootian et al., 2015)
Activated rice husk	Direct red 23	4.35	-	120	10	5-25	(Abdelwahab et al., 2005)
Mahagoni wood coal	Reactive red 120	3.80	3.0	150	10.0	5-70	This study
Alumina/multi-walled carbon nanotubes	Reactive blue 19	3.67	3.0	180	0.40	10–200	(Malakootian et al., 2015)
Clinoptilolite	Reactive red 195	3.18	–	90	–	10–250	(Sismanoglu et al., 2010)
Coconut shell based activated carbon	Reactive blue 19	2.78	–	20	1.0	10–50	(Isah et al., 2015)
Untreated rice husk	Direct Red 23	2.41	-	120	10	5-25	(Abdelwahab et al., 2005)
<i>Helianthus annuus</i> hairy roots	Reactive red 120	1.51	7.0	–	5.0	20–110	(Srikantan et al., 2018)

CONCLUSION

This study investigated the suitability of MWC and MBC as an adsorbent for RR 120 removal in batch adsorption experiments with various controlling parameters like contact time, pH, initial dye concentration, and adsorbent dose. The result reveals that the RR 120 removal efficiency of both adsorbents (MWC and MBC) was increased with the increase of adsorbent dose. The maximum removal was found at pH 3. The Langmuir and Freundlich isotherm had better fit with the experimental data as well as maximum adsorption capacity of 3.806 and 5.402 mg/g for MWC and MBC, respectively. FTIR and SEM results revealed that different functional groups and available pore space on the adsorbent surface may be responsible for RR 120 adsorption. Kinetic studies represented that the adsorption process followed the pseudo-second-order kinetic model with multi-steps diffusion process for both adsorbents (MWC and MBC). Due to low cost, availability, and favorable study result make the MWC and MBC a promising and effective adsorbent for removing RR 120 from aqueous solutions. Consequently, MWC and MBC could be applied for the treatment of textile dye-containing industrial wastewater, where centralized wastewater treatment system is not accessible.

ACKNOWLEDGEMENTS

The authors would like to thank the department of Environmental Science and Technology, Jashore University of Science and Technology for laboratory facilities and reviewers for their valuable comments.

GRANT SUPPORT DETAILS

The present research has been financially supported by The World Academy of Science (TWAS) for instrumental facility under the COMSTECH-TWAS Joint Research Grants Programme (grant No. TWAS Ref: 13-371 RG/ENG/AS_C; UNISCO FR: 3240279207) and KURITA Water and Environment Foundation for research grant award (grant No.17P037).

CONFLICT OF INTEREST

The authors declare that there is not any conflict of interests regarding the publication of this manuscript. In addition, the ethical issues, including plagiarism, informed consent, misconduct, data fabrication and/ or falsification, double publication and/or submission, and redundancy has been completely observed by the authors.

LIFE SCIENCE REPORTING

No life science threat was practiced in this research.

REFERENCES

- Abdelwahab, O., Nemr, A. E., Sikaily, A. E. and Khaled, A. (2005). Use of rice husk for adsorption of direct dyes from aqueous solution: a case study of Direct F. Scarlet. *Egypt. J. Aquat. Res.*, 31(1); 1-11.
- Abbas, R. A., Farhan, A. A. R., Al Ani, H. N. A. and Nechifor, A. C. (2019). Determination of the optimal condition of direct blue dye removal from aqueous solution using eggshell. *Rev. Chim.*, 70(4); 1108-1113.
- Anastopoulou, I., Pashalidis, I., Hosseini-Bandegharai, A., Giannakoudakis, D. A., Robalds, A., Usman, M., Escudero L. B., Zhou, Y., Colmenares, J. C., Núñez-Delgado, A. and Lima, É. C. (2019). Agricultural biomass/waste as adsorbents for toxic metal decontamination of aqueous solutions. *J. Mol. Liq.*, 295; 111684.
- Ahmad, A. A., Hameed, B. H. and Aziz, N. (2007). Adsorption of direct dye on palm ash: Kinetic and equilibrium modeling. *J. Hazard. Mater.*, 141(1); 70-76.
- Ai, L., Zhang, C., Liao, F., Wang, Y., Li, M., Meng, L. and Jiang, J. (2011). Removal of methylene blue from aqueous solution with magnetite loaded multi-wall carbon nanotube: kinetic, isotherm and mechanism analysis. *J. Hazard. Mater.*, 198; 282-290.
- Arami, M., Limaee, N. Y. and Mahmoodi, N. M. (2008). Evaluation of the adsorption kinetics and equilibrium for the potential removal of acid dyes using a biosorbent. *Chem. Eng. J.*, 139(1); 2-10.
- Arica, M. Y. and Bayramoğlu, G. (2007). Biosorption of Reactive Red-120 dye from aqueous solution by native and modified fungus biomass preparations of *Lentinus sajor-caju*. *J. Hazard. Mater.*, 149(2); 499-507.
- Bansal, M., Singh, D. and Garg, V. K. (2009). A comparative study for the removal of hexavalent chromium from aqueous solution by agriculture wastes' carbons. *J. Hazard. Mater.*, 171(1-3); 83-92.
- Çelekli, A., Ilgun, G. and Bozkurt, H. (2012). Sorption equilibrium, kinetic, thermodynamic, and desorption studies of Reactive Red 120 on *Chara contraria*. *Chem. Eng. J.*, 119; 228-235.
- Çelekli, A., Tanrıverdi, B. and Bozkurt, H. (2011). Predictive modeling of removal of Lanaset Red G on *Chara contraria*; kinetic, equilibrium, and thermodynamic studies. *Chem. Eng. J.*, 169(1-3); 166-172.
- Chahm, T., Martins, B. A. and Rodrigues, C. A. (2018). Adsorption of methylene blue and crystal violet on low-cost adsorbent: waste fruits of *Rapanea ferruginea* (ethanol-treated and H₂SO₄-treated). *Environ. Earth Sci.*, 77(13); 508.

- Chakraborty, T. K., Islam, M. S., Zaman, S., Kabir, A. H. M. E. and Ghosh, G. C. (2020). Jute (*Corchorus olitorius*) stick charcoal as a low-cost adsorbent for the removal of methylene blue dye from aqueous solution. *SN Appl. Sci.*, 2; 765.
- Chen, H., Zhao, J., Wu, J. and Dai, G. (2011). Isotherm, thermodynamic, kinetics and adsorption mechanism studies of methyl orange by surfactant modified silkworm exuviae. *J. Hazard. Mater.*, 192; 246–254.
- Dehghani, M. H., Dehghan, A. and Najafpoor, A. (2017). Removing Reactive Red 120 and 196 using chitosan/zeolite composite from aqueous solutions: Kinetics, isotherms, and process optimization. *J. Ind. Eng. Chem.*, 51; 185-195.
- Deng, H., Lu, J., Li, G., Zhang, G. and Wang X. (2011). Adsorption of methylene blue on adsorbent materials produced from cotton stalk. *Chem. Eng. J.*, 172(1); 326-334.
- Dai, Y., Sun, Q., Wang, W., Lu, L., Liu, M., Li, J., Shengshu, Y., Yue, S., Kexin, Z., Jiayi, X., Wenlei, Z., Zhaoyue, H., Yahan, Y., Yüewen, G., Yanjun, C., Xu, Z., Feng, G. and Zhang, Y. (2018). Utilizations of agricultural waste as adsorbent for the removal of contaminants: A review. *Chemosphere.*, 211; 235-253.
- Duran, C., Ozdes, D., Gundogdu, A. and Senturk, H. B. (2011). Kinetics and isotherm analysis of basic dyes adsorption onto almond shell (*Prunus dulcis*) as a low cost adsorbent. *J. Chem. Eng. Data*, 56(5); 2136-2147.
- Eren, Z. and Acar, F. N. (2006). Adsorption of Reactive Black 5 from an aqueous solution: equilibrium and kinetic studies. *Desalination*, 194(1-3); 1-10.
- Freundlich, H. M. F. (1906). Over the adsorption in solution. *J. Phys. Chem.*, 57; 358-471.
- Ghosh, G. C., Chakraborty, T. K., Zaman, S., Nahar, M. N. and Kabir, A. H. M. E. (2020). Removal of Methyl Orange Dye from Aqueous Solution by a Low-Cost Activated Carbon Prepared from Mahagoni (*Swietenia mahagoni*) Bark. *Pollution*, 6(1); 171-184.
- Ghosh, G. C., Samina, Z., & Chakraborty, T. K. (2018). Adsorptive removal of Cr (VI) from aqueous solution using rice husk and rice husk ash. *Desalin. Water Treat.*, 130; 151-160.
- Gupta, V. K., Pathania, D., Agarwal, S. and Singh, P. (2012). Adsorptional photocatalytic degradation of methylene blue onto pectin-CuSnanocomposite under solar light. *J. Hazard. Mater.*, 243; 179-186.
- Hasan, M. B. and Hammood, Z. A. (2018). Wastewater Remediation via Modified Activated Carbon: A Review. *Pollution*, 4(4); 707-723.
- Ho, Y. S. and McKay, G. (2000). The kinetics of sorption of divalent metal ions onto sphagnum moss peat. *Water Res.*, 34(3); 735-742.
- Ip, A. W. M., Barford, J. P. and McKay, G. (2009). Reactive Black dye adsorption/desorption onto different adsorbents: effect of salt, surface chemistry, pore size and surface area. *J. Colloid. Interface Sci.*, 337(1); 32-38.
- Isah, U., Abdurraheem, G., Bala, S., Muhammad, S. and Abdullahi, M. (2015). Kinetics, equilibrium and thermodynamics studies of C.I. Reactive Blue 19 dye adsorption on coconut shell based activated carbon. *Int. Biodeter. Biodegr.*, 102; 265-273.
- Jain, M., Garg, V. K. and Kadirvelu, K. (2010). Adsorption of hexavalent chromium from aqueous medium onto carbonaceous adsorbents prepared from waste biomass. *J. Environ.*, 99(4); 949-957.
- Kadirvelu, K., Kavipriya, M., Karthika, C., Radhika, M., Vennilamani, N. and Pattabhi, S. (2003). Utilization of various agricultural wastes for activated carbon preparation and application for the removal of dyes and metal ions from aqueous solutions. *Bioresour. Technol.*, 87(1); 129-132.
- Khattari, S. D. and Singh, M. K. (2000). Colour removal from synthetic dye wastewater using a bioadsorbent. *Water Air Soil Pollut.*, 120(3-4); 283-294.
- Kumar, K. V., Ramamurthi, V. and Sivanesan, S. (2005). Modeling the mechanism involved during the sorption of methylene blue onto fly ash. *J. Colloid. Interface Sci.*, 284(1); 14-21.
- Lagergren, S. (1898). About the theory of so-called adsorption of soluble substances. *Kungliga Svenska Vetenskapsakademiens Handlingar.*, 24(4); 1-39.
- Langmuir, I. (1917). The constitution and fundamental properties of solids and liquids. II. Liquids. *J. Am. Chem. Soc.*, 39(9); 1848-1906.

- Mahmoodi, N. M., Hayati, B., Arami, M. and Lan, C. (2011). Adsorption of textile dyes on Pine cone from colored wastewater: kinetic, equilibrium and thermodynamic studies. *Desalination*, 268(1-3); 117-125.
- Malakootian, M., Mansooria, H. J., Hosseini, A. and Khanjani, N. (2015). Evaluating the efficacy of alumina/carbon nanotube hybrid adsorbents in removing Azo Reactive Red 198 and Blue 19 dyes from aqueous solutions. *Process Saf. Environ.*, 96; 125-137.
- Mubarak, N. S. A., Jawad, A. H. and Nawawi, W. I. (2017). Equilibrium, kinetic and thermodynamic studies of Reactive Red 120 dye adsorption by chitosan beads from aqueous solution. *Energ. Ecol. Environ.*, 2(1); 85-93.
- Munagapati, V. S., Yarramuthi, V. and Kim, D. S. (2017). Methyl orange removal from aqueous solution using goethite, chitosan beads and goethite impregnated with chitosan beads. *J. Mol. Liquids.*, 240; 329-339.
- Munagapati, V. S., Yarramuthi, V., Kim, Y., Lee, K. M. and Kim, D. S. (2018). Removal of anionic dyes (Reactive Black 5 and Congo Red) from aqueous solutions using Banana Peel Powder as an adsorbent. *Ecotoxicol. Environ.*, 148; 601-607.
- Naveen, N., Saravanan, P., Baskar, G. and Renganathan, S. (2011). Equilibrium and kinetic modeling on the removal of Reactive Red 120 using positively charged *Hydrilla verticillata*. *J. Taiwan Inst. Chem. E.*, 42(3); 463-469.
- Ngah, W. S. W. and Musa, A. (1998). Adsorption of humic acid onto chitin and chitosan. *J. Appl. Polym. Sci.*, 69(12); 2305-2310.
- Panda, G. C., Das, S. K. and Guha, A. K. (2009). Jute stick powder as a potential biomass for the removal of congo red and rhodamine B from their aqueous solution. *J. Hazard. Mater.*, 164(1); 374-379.
- Qian, W. C., Luo, X. P., Wang, X., Guo, M. and Li, B. (2018). Removal of methylene blue from aqueous solution by modified bamboo hydrochar. *Ecotoxicol. Environ. Saf.*, 157; 300-306.
- Robinson, T., McMullan, G., Marchant, R. and Nigam, P. (2001). Remediation of dyes in textile effluent: a critical review on current treatment technologies with a proposed alternative. *Bioresour. Technol.*, 77(3); 247-255.
- Rusmin, R., Sarkar, B., Liu, Y., McClure, S. and Naidu, R. (2015). Structural evolution of chitosan-palygorskite composites and removal of aqueous lead by composite beads. *Appl. Surf. Sci.*, 353; 363-375.
- Rápó, E., Szép, R., Keresztesi, Á., Suciú, M. and Tonk, S. (2018). Adsorptive removal of cationic and anionic dyes from aqueous solutions by using eggshell household waste as biosorbent. *Acta Chim. Slov.*, 65(3); 709-717.
- Shirmardi, M., Mesdaghinia, A., Mahvi, A. H., Nasser, S. and Nabizadeh, R. (2012). Kinetics and equilibrium studies on adsorption of acid red 18 (Azo-Dye) using multiwall carbon nanotubes (MWCNTs) from aqueous solution. *J. Chem.*, 9(4); 2371-2383.
- Sismanoglu, T., Kismir, Y. and Karakus, S. (2010). Single and binary adsorption of reactive dyes from aqueous solutions onto clinoptilolite. *J. Hazard. Mater.*, 184(1-3); 164-169.
- Srikantan, C., Suraishkumar, G. K. and Srivastava, S. (2018). Effect of light on the kinetics and equilibrium of the textile dye (Reactive Red 120) adsorption by *Helianthus annuus* hairy roots. *Bioresour. Technol.*, 257; 84-91.
- Subbaiah, M. V. and Kim, D. S. (2016). Adsorption of methyl orange from aqueous solution by aminated pumpkin seed powder: Kinetics, isotherms, and thermodynamic studies. *Ecotoxicol. Environ. Safety.*, 128; 109-117.
- Subramani, S. E. and Thinakaran, N. (2017). Isotherm, kinetic and thermodynamic studies on the adsorption behaviour of textile dyes onto chitosan. *Process Saf. Environ. Protec.*, 106; 1-10.
- Weber, W. J. and Morris, J. C. (1963). Kinetics of adsorption on carbon from solution. *J. Sanit. Eng. Div.*, 89(2); 31-60.
- Yagub, M. T., Sen, T. K., Afroze, S. and Ang, H. M. (2014). Dye and its removal from aqueous solution by adsorption: a review. *Adv. Colloid. Interface Sci.*, 209; 172-184.
- Yaman, M. and Demirel, M. H. (2020). Synthesis and characterization of activated carbon from biowaste-walnut shell and application to removal of uranium from waste. *Pollution.*, 6(4); 935-944.

- Zhang, Z., O'Hara, I. M., Kent, G. A. and Doherty, W. O. (2013). Comparative study on adsorption of two cationic dyes by milled sugarcane bagasse. *Ind. Crop. Prod.*, 42; 41-49.
- Zheng, L., Wang, C., Shu, Y., Yan, X. and Li, L. (2015). Utilization of diatomite/chitosan-Fe (III) composite for the removal of anionic azo dyes from wastewater: equilibrium, kinetics and thermodynamics. *Colloids Surf. A: Physicochem Eng. Asp.*, 468; 129-139.
- Zhu, X., Liu, Y., Qian, F., Zhou, C., Zhang, S. and Chen, J. (2015). Role of hydrochar properties on the porosity of hydrochar-based porous carbon for their sustainable application. *ACS Sustain. Chem. Eng.*, 3(5); 833-840.